Applied Mathematics & Information Sciences
An International Journal

http://dx.doi.org/10.18576/amis/100619

Hydromagnetic Peristaltic Transport of Variable Viscosity Fluid with Heat Transfer and Porous Medium

F. M. Abbasi[1,2,*], *T. Hayat*[2,3] *and B. Ahmad*[3].

[1] Department of Mathematics, COMSATS Institute of Information Technology, Islamabad 44000, Pakistan.
[2] Department of Mathematics, Quaid-I-Azam University 45320, Islamabad 44000, Pakistan.
[3] Nonlinear Analysis and Applied Mathematics (NAAM) Research Group, Faculty of Science, King Abdulaziz University, Jeddah 21589, Saudi Arabia.

Received: 9 Jul. 2016, Revised: 11 Sep. 2016, Accepted: 17 Sep. 2016
Published online: 1 Nov. 2016

Abstract: This article examines the peristaltic transport of variable viscosity fluid in a planar channel with heat transfer. The fluid viscosity is taken temperature dependent. The fluid is electrically conducting in the presence of a constant applied magnetic field. Both channel and magnetic field possess the inclined considerations. An incompressible fluid saturates the porous space. Heat transfer analysis is carried out in the presence of viscous dissipation and Joule heating. The resulting problems are solved numerically. A parametric study is performed to predict the impact of embedded variables. Results indicate that the fluid with variable viscosity has higher value of pressure gradient compared with that of constant viscosity fluid. Size of the trapped bolus increases with an increase in viscosity and permeability parameters. Constant viscosity fluid possesses lower velocity near the center of channel when compared with variable viscosity fluid. Effects of porous medium on pressure gradient and velocity are qualitatively similar.

Keywords: Peristaltic transport; Temperature dependent viscosity; Magnetohydrodynamics (MHD); Porous medium; Joule heating.

1 Introduction

The peristaltic transport of fluid caused by a progressive wave of area contraction/expansion along the length of a distensible tube has received growing interest of the recent researchers. To a large extent, such interest is stimulated by the fact that peristaltic activity is involved in practical applications of physiological and industrial processes. These include the locomotion of worms, urine passage from kidney to bladder, food swallowing by the esophagus, vasomotion of small blood vessels, sanitary and corrosive fluids transport, movement of bio fluids (chyme in gastrointestinal tract, bile in the bile duct, ovum in the fallopian tube and spermatozoa in cervical canal) and in heart lung machine and roller and finger pumps. Latham [1] was the first who studied experimentally the mechanism of peristalsis for flow of viscous fluids. Afterwards, several researchers examined the peristalsis subject to various assumptions through theoretical and experimental attempts. Available information on the topic for peristalsis of viscous and non-Newtonian fluids [2,3,4,5] at present is impressive and we here only refer few recent studies in this direction [6,7,8,9,10,11,12,13,14].

The porous medium and heat transfer effects are quite important in the biological tissue. Especially such considerations are significant in blood flow simulation related to tumors and muscles, drugs transport, production of osteoinductive material, nutrients to brain cells etc. Moreover, the flow models with magnetic field have numerous applications in cross field accelerators, pumps, flow meters and MHD generators. In such devices, the flow is subjected to heat that dissipated internally by viscous/Joule heating or that produced due to electric currents in the walls. The peristaltic transport of MHD fluid has interaction with problems of movement of the conductive physiological fluids, e.g. the blood and blood pump machines. The peristalsis with heat transfer is further prominent in oxygenation and hemodialysis processes. With this importance in mind, Srinivas and Muthuraj [15] addressed the effects of heat transfer in peristaltic flow of viscous fluid saturating porous medium. Srinivas and Kothandapani [16] addressed the heat transfer analysis in peristaltic flow by complaint

* Corresponding author e-mail: abbasisarkar@gmail.com

walls. Abd elmaboud and Mekheimer [17] discussed the peristaltic transport of second order fluid in a porous space. Mekheimer [18] investigated the nonlinear peristaltic transport through a porous medium in an inclined planar channel. The effects of magnetic field and space porosity on compressible Maxwell fluid were studied by Mekheimer et al. [19]. Tripathi [20] analyzed the transient peristaltic heat flow in a finite porous channel. Influence of heat transfer on peristaltic flow of an electrically conducting fluid through porous medium has been addressed by Hayat et al. [21]. The interaction of peristaltic motion with heat transfer in planar and curved flow configurations has been explored in the studies [21,22,23,24,25,26,27].

Existing information on the topic reveals that no attention has been given so far to the peristaltic flow of variable viscosity fluid through an inclined channel and inclined applied magnetic field. The objective of present communication is to address this problem in the presence of viscous dissipation and Joule heating effects. The problem is modeled when an incompressible fluid fills the porous medium. Numerical solution is given after utilizing the long wavelength and low Reynolds number concept. Physical quantities of interest are analyzed for the pertinent parameters entering into problem statement.

2 Mathematical analysis

Let us examine the peristaltic transport of an incompressible viscous fluid in a symmetric channel. The channel is taken inclined at an angle α to the vertical. The fluid is electrically conducting in the presence of an inclined magnetic field with constant strength $\mathbf{B}_0$. Applied/induced electric fields are absent. Further the effects of induced magnetic fields are ignored subject to low magnetic Reynolds number approximation. The flow generated is due to peristaltic waves travelling along the channel walls. Schematic diagram of the geometry is given in Fig. A.

Mathematically the wall geometry is chosen in the form

$$\overline{H}(\overline{X},\overline{t}) = a+\varepsilon,$$

where a is the half channel width and ε is the disturbance produced due to propagation of peristaltic waves at the walls. This disturbance can be written in the form

$$\varepsilon = bcos\left(\frac{2\pi}{\lambda}(\overline{X}-c\overline{t})\right),$$

in which $\overline{t}$ is time, b is the amplitude of the peristaltic wave, c and λ are the speed and wavelength of the waves respectively. Appropriate velocity field for this problem is $\overline{V} = \left[U(\overline{X},\overline{Y},\overline{t}),V(\overline{X},\overline{Y},\overline{t}),0\right]$. Here $\overline{U}$, $\overline{V}$ and $\overline{P}$ are the velocity components and pressure in the laboratory frame $(\overline{X},\overline{Y},\overline{t})$. We further adopt $(\overline{u},\overline{v})$ and $\overline{p}$ as the velocity components and pressure in the wave frame $(\overline{x},\overline{y})$. The transformations between laboratory and wave frames are

$$\overline{x} = \overline{X}-c\overline{t},\ \ \overline{y} = \overline{Y},\ \ \overline{u} = \overline{U}-c,\ \ \overline{v} = \overline{V},\ \ \overline{p}(\overline{x},\overline{y}) = \overline{P}(\overline{X},\overline{Y},\overline{t}). \tag{1}$$

The governing equations in the wave frame are given by

$$\frac{\partial\overline{u}}{\partial\overline{x}}+\frac{\partial\overline{v}}{\partial\overline{y}} = 0, \tag{2}$$

$$\begin{aligned}\rho\left((\overline{u}+c)\frac{\partial}{\partial\overline{x}}+\overline{v}\frac{\partial}{\partial\overline{y}}\right)(\overline{u}+c) = {} & -\frac{\partial\overline{p}}{\partial\overline{x}}+2\frac{\partial}{\partial\overline{x}}\left(\overline{\mu}(T)\frac{\partial\overline{u}}{\partial\overline{x}}\right)+\frac{\partial}{\partial\overline{y}}\left[\overline{\mu}(T)\left(\frac{\partial\overline{v}}{\partial\overline{x}}+\frac{\partial\overline{u}}{\partial\overline{y}}\right)\right] \\ & -\sigma B_0^2 Cos\beta\left((\overline{u}+c)Cos\beta-\overline{v}Sin\beta\right)+\rho g\alpha^*\left(T-T_0\right)Sin\alpha+\rho gSin\alpha-\frac{\overline{\mu}(T)(\overline{u}+c)}{\overline{k}},\end{aligned} \tag{3}$$

$$\begin{aligned}\rho\left((\overline{u}+c)\frac{\partial}{\partial\overline{x}}+\overline{v}\frac{\partial}{\partial\overline{y}}\right)(\overline{v}) = {} & -\frac{\partial\overline{p}}{\partial\overline{y}}+2\frac{\partial}{\partial\overline{y}}\left(\overline{\mu}(T)\frac{\partial\overline{v}}{\partial\overline{y}}\right)+\frac{\partial}{\partial\overline{x}}\left[\overline{\mu}(T)\left(\frac{\partial\overline{v}}{\partial\overline{x}}+\frac{\partial\overline{u}}{\partial\overline{y}}\right)\right] \\ & -\sigma B_0^2 Sin\beta\left((\overline{u}+c)Cos\beta-\overline{v}Sin\beta\right)-\rho g\alpha^*\left(T-T_0\right)Cos\alpha-\rho gCos\alpha-\frac{\overline{\mu}(T)(\overline{v})}{\overline{k}},\end{aligned} \tag{4}$$

$$\begin{aligned}\rho C_p\left((\overline{u}+c)T_{\overline{x}}+\overline{v}T_y\right) = {} & K\left[T_{\overline{xx}}+T_{\overline{yy}}\right]+\overline{\mu}(T)\left[2\left\{\left(\frac{\partial\overline{u}}{\partial\overline{x}}\right)^2+\left(\frac{\partial\overline{v}}{\partial\overline{y}}\right)^2\right\}+\left(\frac{\partial\overline{v}}{\partial\overline{x}}+\frac{\partial\overline{u}}{\partial\overline{y}}\right)^2\right] \\ & +\sigma B_0^2\left((\overline{u}+c)Cos\beta-\overline{v}Sin\beta\right)^2+\frac{\overline{\mu}(T)(\overline{u}+c)^2}{\overline{k}},\end{aligned} \tag{5}$$

in which ρ is the density of fluid, μ is the dynamic viscosity, g is the acceleration due to gravity, $\overline{k}$ is permeability of the porous medium parameter, β is the inclination of applied magnetic field and α^* is the thermal expansion coefficient. The additional viscous dissipation term in the energy equation accounts effect in limits of small and large permeability of porous medium. We also denote C_p as the specific heat, K the thermal conductivity and T the temperature of the fluid.

The long wave length approximation is widely used in the analysis of peristaltic flows [29]. Such approximation makes use of the fact that the wavelength of peristaltic wave is considerably large when compared with the half width of the channel/tube. These considerations are relevant for the case of chyme transport through small intestine [6] where $a = 1.25cm$ and $\lambda = 8.01cm$. Clearly half width of the intestine is small in comparison to the wavelength of peristaltic wave i.e. $a/\lambda = 0.156$. Further, Lew et al. [7] concluded that Reynolds number for the fluid mechanics in small intestine is small. Making use of the following dimensionless quantities.

Defining the dimensionless quantities

$$\begin{aligned} x &= \frac{\overline{x}}{\lambda},\ y=\frac{\overline{y}}{a},\ u=\frac{\overline{u}}{c},\ v=\frac{\overline{v}}{c\delta},\ \delta=\frac{a}{\lambda},\ h=\frac{\overline{H}}{a},\ d=\frac{b}{a},\ p=\frac{a^2\overline{p}}{c\lambda\mu_0},\ \upsilon=\frac{\mu_0}{\rho}, \\ \mu(\theta) &= \frac{\overline{\mu}(T)}{\mu_0},\ M^2=\left(\frac{\sigma}{\mu_0}\right)^2 B_0^2a^2,\ Re=\frac{\rho ca}{\mu_0},\ t=\frac{c\overline{t}}{\lambda},\ \theta=\frac{T-T_0}{T_0},\ Gr=\frac{\rho g\alpha^* T_0 a^2}{\mu_0 c}, \\ Fr &= \frac{c^2}{ga},\ k=\frac{\overline{k}}{a^2},\ Br=\mathrm{Pr}E,\ E=\frac{c^2}{C_pT_0},\ Pr=\frac{\mu_0 C_p}{K},\ u=\psi_y,\ v=-\psi_x,\end{aligned} \tag{6}$$

and adopting long wavelength and low Reynolds number approach, the equations in terms of stream function ψ are

$$\begin{aligned}\frac{\partial p}{\partial x} = {} & \frac{\partial}{\partial y}\left[\mu(\theta)\frac{\partial^2\psi}{\partial y^2}\right]-\left\{M^2Cos^2\beta+\frac{\mu(\theta)}{k}\right\}\left(\frac{\partial\psi}{\partial y}+1\right)+ \\ & Gr\theta Sin\alpha+\frac{ReSin\alpha}{Fr},\end{aligned} \tag{7}$$

$$\frac{\partial p}{\partial y} = 0, \tag{8}$$

$$\frac{\partial^2\theta}{\partial y^2}+Br\mu(\theta)(\psi_{yy})^2+Br\left[M^2Cos^2\beta+\frac{\mu(\theta)}{k}\right]\left(\frac{\partial\psi}{\partial y}+1\right)^2 = 0, \tag{9}$$

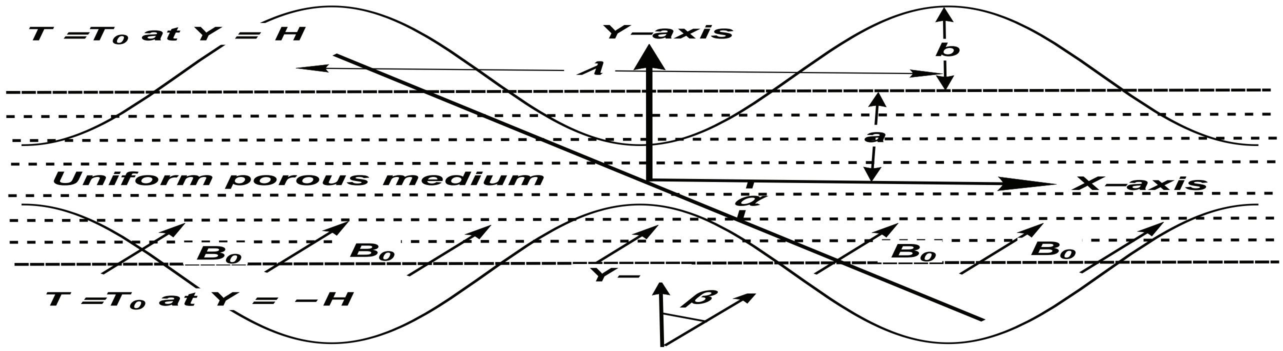

Figure A: Geometry of the problem.

Note that the incompressibility condition is automatically satisfied and Eq. (8) witnesses that $p \neq p(y)$. From Eqs. (7) and 8 we have

$$0=\frac{\partial^2}{\partial y^2}\left[\mu(\theta)\frac{\partial^2\psi}{\partial y^2}\right]-\left\{M^2Cos^2\beta+\frac{\mu(\theta)}{k}\right\}\left(\frac{\partial^2\psi}{\partial y^2}\right)+Gr\frac{\partial\theta}{\partial y}Sin\alpha. \quad (10)$$

Here υ denotes the kinematic viscosity, Re the Reynolds number, Br the Brinkman number, E the Eckret number, Pr the Prandtl number, δ the wave number, Gr the Grashoff number, Fr the Froud number, k the dimensionless permeability parameter and θ the dimensionless temperature.

We consider the temperature dependent viscosity in the form [24]

$$\mu(\theta)=e^{-\gamma\theta}$$

which gives

$$\mu(\theta)=1-\gamma\theta, \quad \text{for } \gamma \ll 1.$$

where γ is the viscosity parameter. Note that for $\gamma=0$ our problem reduces for the constant viscosity case i.e. for the case when the viscosity does not depend upob temperature [28,29].

Defining η and F as the dimensionless mean flows in the laboratory and wave frames we have

$$\eta=F+1 \quad (11)$$

where

$$F=\int_0^h\frac{\partial\psi}{\partial y}dy. \quad (12)$$

The corresponding boundary conditions for the present flow configuration are

$$\psi=0, \quad \frac{\partial^2\psi}{\partial y^2}=0, \quad \frac{\partial\theta}{\partial y}=0, \quad y=0,$$
$$\psi=F, \ \frac{\partial\psi}{\partial y}=-1, \ \theta=0, \ y=h, \quad (13)$$

with

$$h(x)=1+d\cos(2\pi x). \quad (14)$$

3 Results and discussion

Numerical solutions of the derived problems are obtained. For that we have taken 0.01 as the step size for variation of x and y. The obtained results are analyzed graphically here.

The graphs of pressure gradient, stream function, velocity and temperature are examined. Moreover, the numerical values of heat transfer rate at the wall are computed and analyzed through Table 1. Hence Figs. 1 (a-h) are plotted to analyze the pressure gradient variation with various embedded parameters. Figs. 2-8 depict the behavior of streamlines, Figs. 9 (a-f) for velocity and Figs. 10 (a-f) for the temperature profile.

It is seen that the pressure gradient varies and has maximum value at the wider part of the channel. Minimum value of the pressure gradient is found near the more occlude part of the channel. It is observed that value of the pressure gradient increases with an increase in the variable viscosity parameter i.e. the pressure gradient has a higher value for the variable viscosity fluid than that of the fluid with constant viscosity (see Fig. 1 a). Presence of porous medium decreases the value of pressure gradient (see Fig. 1 b). As we move from the horizontal to the vertical channel, pressure gradient attains higher value. Increase in the Hartman number and decrease in the magnetic field inclination tend to decrease the pressure gradient (Figs. 1 d and f). An increase in Froud number decreases the pressure gradient while the Brinkman number increases its value (Figs. 1 e and h). Corresponding value of the pressure gradient is higher in the case of resisting flow when compared to that of the assisting flow (Fig. 1 g).

The volume of the fluid trapped within a streamline is usually termed as bolus. This study showed that the size of the trapped bolus decreases with an increase in the magnetic field parameter M (see Fig. 2). Bolus size is found to be small in the case of fluid with constant viscosity (see Fig. 3). Size of the trapped bolus increases with an increase in the value of the porosity parameter k. It means that the bolus size gets reduced in case of flow through porous medium (Fig. 4). From Fig. 5 it is observed that an increase in the channel inclination angle decreases the size of the trapped bolus. It is further noted that the effect of channel inclination angle on the size of bolus largely depends on the value of Grashoff number. For small values of Grashoff number the size of trapped bolus is almost unaltered for change in channel inclination angle. On the other hand for large values of Grashoff number the bolus size decreases by increasing the channel inclination angle. Increase in the magnetic field inclination angle and the Brinkman number result in an increase in the size of trapped bolus (see Figs. 6 and 7). Bolus is found to have a comparatively large size in the case of assisting flow (+ value of g) (see Fig. 8). This is mainly due to the fact that magnetic field inclination angle when increased results in a decrease in the retarding effect of the Lorentz force and for zero channel inclination angle the applied magnetic field has maximum influence on the flow. Velocity profile is seen to follow a parabolic trajectory with maximum value near the center of the channel. Such value of the velocity increases when we move from constant viscosity fluid to the fluid with temperature dependent viscosity. It is seen from Fig. 9b that the velocity decreases in the case of porous medium. Increase in the Hartman number decreases the velocity near the center line whereas the case is opposite for an increase in Brinkman number (see Figs. 9 d and f). Inclination of the channel results in the increase of the velocity for both assisting and resisting flows (see Fig. 9 c). Fig. 9 e revealed that the velocity has a higher value for assisting flow.

Dimensionless temperature is analyzed in the Figs. 10 (a-f). Fig. 10 showed that the temperature is higher for the case of constant viscosity fluid when compared with the fluid of variable viscosity. It is found from Fig. 10 that an increase in the value of permeability parameter decreases the value of the dimensionless temperature. Dimensionless temperature increases with an increase in the value of the Hartman number (Fig. 10 c). Similarly temperature is higher for the case of assisting flow (see Fig. 10 d). Increase in inclination of channel gives higher value of the temperature whereas the case is opposite for the inclination of magnetic field (see Figs. 10 e and f).

Numerical values of the heat transfer rate at the wall for different parameters are plotted in Table 1. It is noted that the heat transfer rate decreases by increasing the viscosity parameter γ, permeability parameter k, Grashoff number G_r and channel and magnetic field inclinations (α and β respectively). However it increases due to increase in Hartman number (M) and Brinkman number Br. The used values of the parameters here are $\gamma = 0.2, k = 1.0, \alpha, \beta = \pi/4, Re = 5, Fr = 2, Br = 0.5, M = 0.5, Gr = 0.5, d = 0.3$ and $\eta = 0.3$.

4 Concluding remarks

Numerical analysis for the peristaltic transport of variable viscosity fluid with porous medium and heat transfer in an inclined channel is carried out. Results indicate that the pressure gradient has a higher value for variable viscosity fluid than constant viscosity fluid. Decrease in the pressure gradient in presence of porous medium is observed. It is seen that the pressure gradient has higher value when channel is vertical and there is resisting flow. Size of the trapped bolus increases with an increase in viscosity and permeability parameters. Trapped bolus has a larger size for assisting flow case. Fluid with constant viscosity possesses lower velocity near the center of the channel when compared with that of fluid with variable viscosity. The effects of porous medium on pressure gradient and velocity are qualitatively similar. Unlike velocity, temperature of the fluid is higher for constant viscosity case. Further the temperature is higher for the case of assisting flow. Heat transfer rate at the wall decreases with an increase in channel and magnetic field inclination angles.

Table 1. Numerical values of heat transfer rate at the wall for different parameters.

γ	k	M	G_r	α	β	Br	$\theta'(h)$
0.0	1.0	1.0	2	$\pi/4$	$\pi/4$	0.5	2.32081
0.3							1.76871
0.6							1.44276
0.2	0.5						2.24094
	2.0						1.71568
	10.0						1.52373
	1.0	0.0					1.61917
		1.0					1.91839
		2.0					2.8159
		1.0	−2.0				1.95425
			0.0				1.93242
			2.0				1.91839
			1.0	0.0			1.93242
				$\pi/4$			1.92427
				$\pi/2$			1.92153
				$\pi/4$	0.0		2.22499
					$\pi/4$		1.92427
					$\pi/2$		1.62345
					$\pi/4$	0.1	0.401872
						0.2	0.795321
						0.3	1.18027

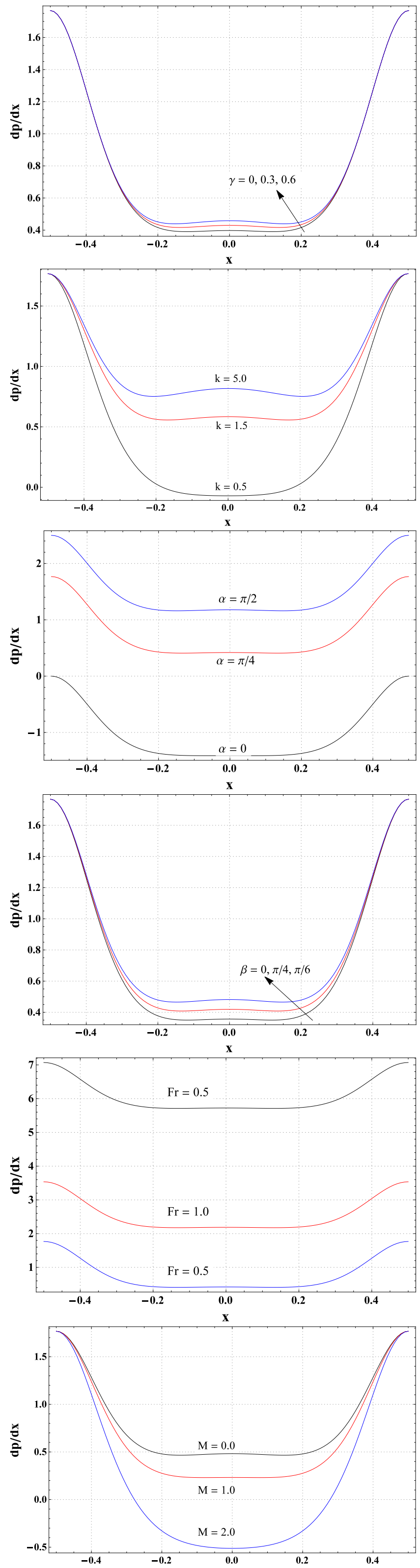

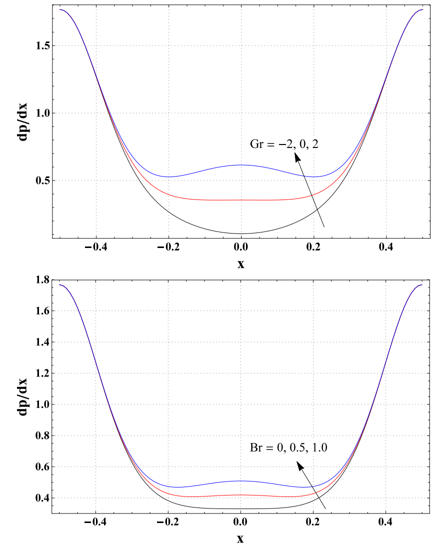

Fig. 1 (a-h) Pressure gradient for the various parameters

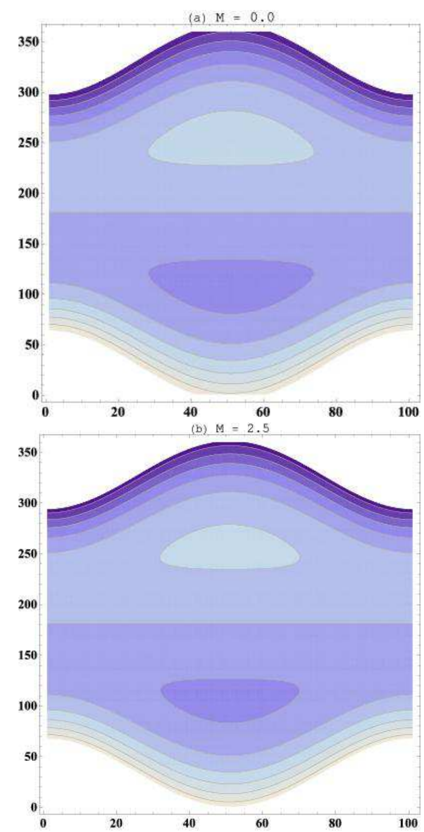

Fig. 2 Streamlines for variation of Hartman number.

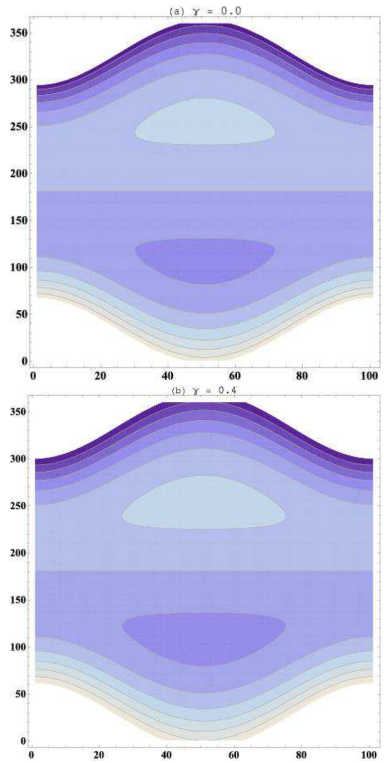

Fig. 3 Streamlines for variation of viscosity parameter.

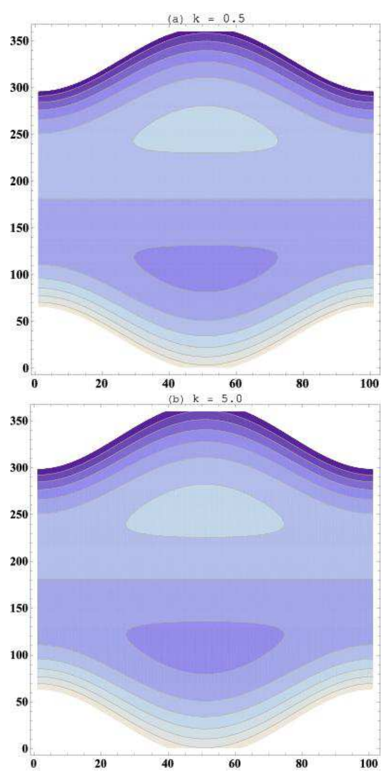

Fig. 4 Streamlines for variation of porosity parameter.

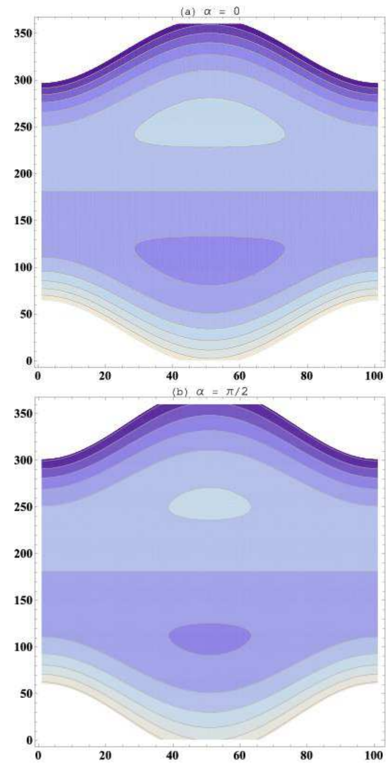

Fig. 5 Streamlines for variation of channel inclination.

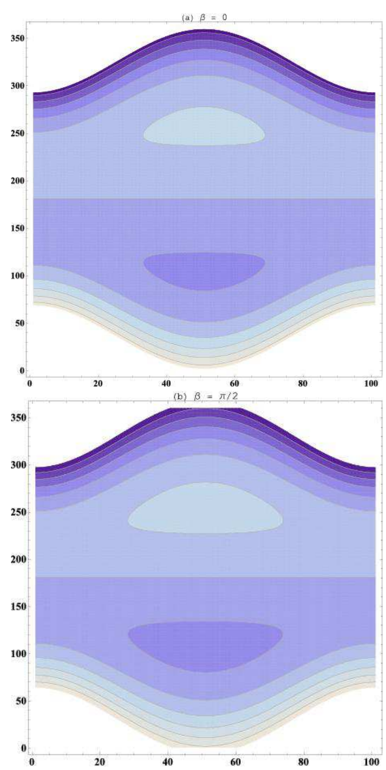

Fig. 6 Streamlines for different inclinations of magnetic field.

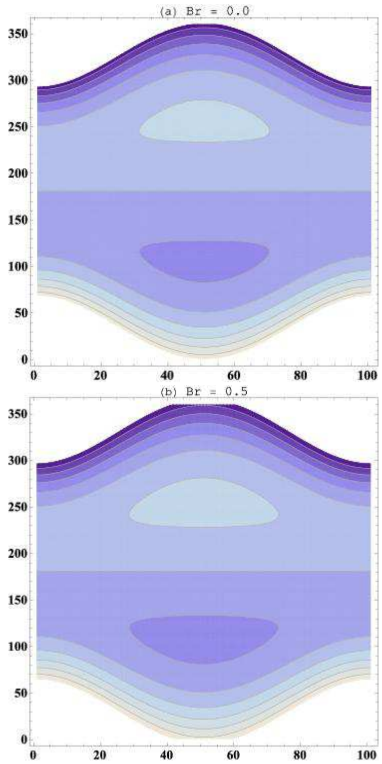

Fig. 7 Streamlines for different Brinkman number.

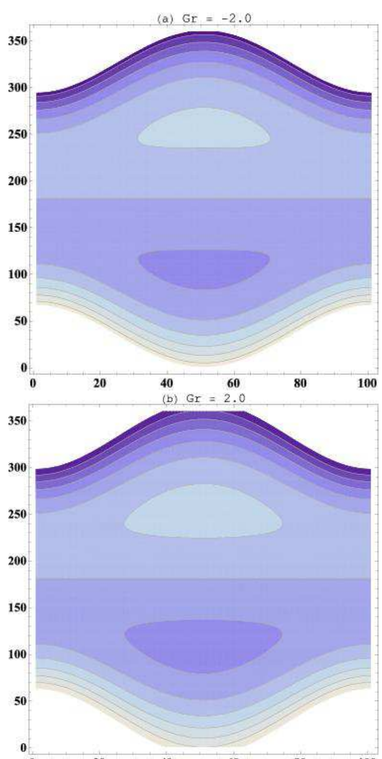

Fig. 8 Streamlines for different Grashoff number.

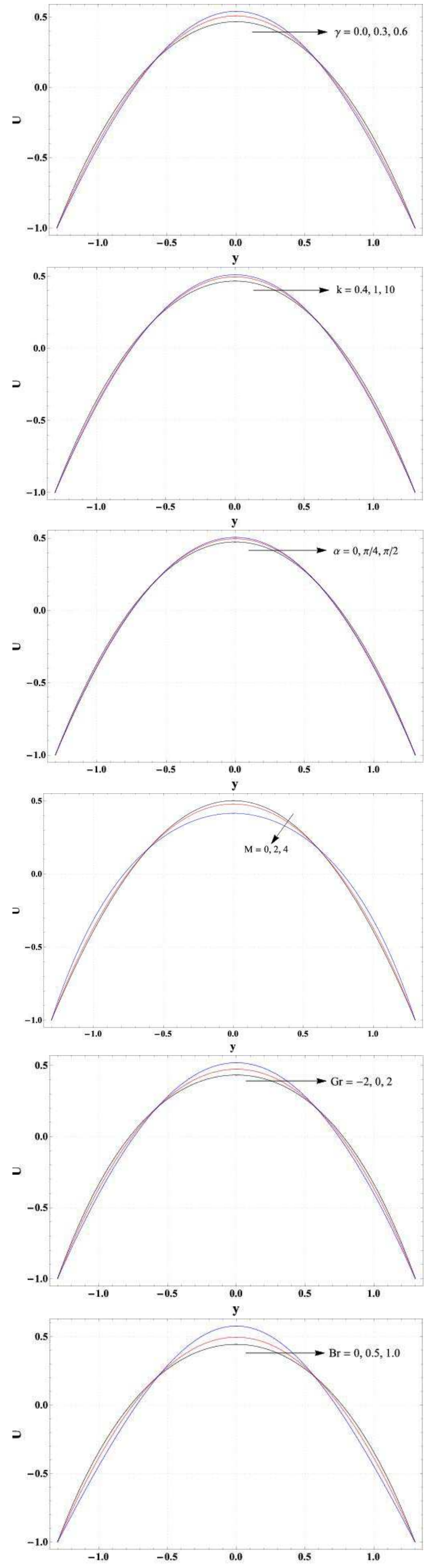

Fig. 9 (a-f) Velocity profile for different parameter.

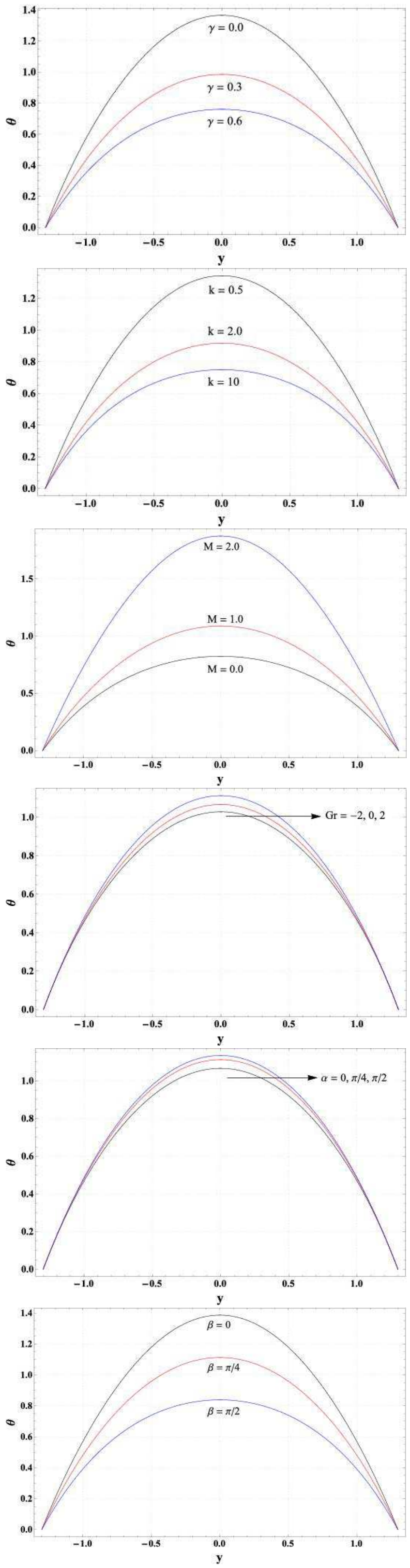

Fig. 10 (a-f) Temperature profile for different parameters.

References

[1] T. W. Latham, Fluid motion in a peristaltic pump, M. S. Thesis, Massachusetts Institute of technology, Cambridge, MA, (1966).

[2] M. Jamil, C. Fetecau and M. Imran, Unsteady helical flows of Oldroyd-B fluids, Commun. Nonlinear Sci. Numer. Simulat., 16, 1378-1386 (2011).

[3] M. Jamil, A. Rauf, C. Fetecau and N.A. Khan, Helical flows of second grade fluid due to constantly accelerated shear stresses, Commun. Nonlinear Sci. Numer. Simulat., 16, 1959-1969 (2011).

[4] S. Wang and W. C. Tan, Stability analysis of soret-driven double-diffusive convection of Maxwell fluid in a porous medium, Int. J. Heat Fluid Flow, 32, 88-94 (2011).

[5] T. Hayat, S. A. Shehzad, M. Qasim and S. Obaidat, Steady flow of Maxwell fluid with convective boundary conditions, Z. Naturforsch. A, 66a, 417-422 (2011).

[6] L.M. Srivastava and V. P. Srivastava, Peristaltic transport of a power law fluid: Applications to the ductus efferentes of the reproductive tract, Rheol. Acta., 27, 428-433 (1988).

[7] S. H. Lew, Y. C. Fung and C. B. Lowenstein, Peristaltic carrying and mixing of chyme. J. Biomech., 4, 297-315 (1971).

[8] Kh.S. Mekheimer, Non- linear peristaltic transport of MHD flow in an inclined planar channel, Arabian J. Sci. Engin., 28, 183-201 (2003).

[9] Kh.S. Mekheimer, Effect of the induced magnetic field on peristaltic flow of a couple stress fluid, Physics Letters A, 372, 4271-4278 (2008).

[10] Kh.S. Mekheimer and Y. Abd elmaboud, Peristaltic flow of a couple stress fluid in an annulus: Application of an endoscope, Physica A: Stat. Mech. App., 387, 2403-2415 (2008).

[11] M. Kothandapani and S. Srinivas, Peristaltic transport of a Jeffrey fluid under the effect of magnetic field in an asymmetric channel, Int. J. Non-Linear Mech. 43, 915-924 (2008).

[12] F. M. Abbasi, A. Alsaedi, and T. Hayat, Peristaltic transport of Eyring-Powell fluid in a curved channel, J. Aerosp. Eng., 27, 04014037 (2014).

[13] T. Hayat, F. M. Abbasi, B. Ahmad and A. Alsaedi, Peristaltic transport of Carreau-Yasuda fluid in a curved channel with slip effects, PLoS ONE 9(4), e95070 (2014).

[14] F. M. Abbasi, T. Hayat and A. Alsaedi, Numerical analysis for MHD peristaltic transport of Carreau-Yasuda fluid in a curved channel with Hall effects, J. Magnetism and Magnetic Materials, 382 (2015) 104–110.

[15] S. Srinivas and R. Muthuraj, Effects of chemical reaction and space porosity on MHD mixed convective flow in a vertical asymmetric channel with peristalsis, Math. Comp. Mod., 54, 1213-1227 (2011).

[16] S. Srinivas and M. Kothandapani, The influence of heat and mass transfer on MHD peristaltic flow through a porous space with compliant walls, App. Math. Comp., 213, 197-208 (2009).

[17] Y. Abd elmaboud and Kh.S. Mekheimer, Non-linear peristaltic transport of a second-order fluid through a porous medium, App. Math. Mod., 35, 2695-2710 (2011).

[18] Kh.S. Mekheimer, Non-linear peristaltic transport through a porous medium in an inclined planar channel, J. Porous Media, 6, 190-202 (2003).

[19] Kh. S. Mekheimer, S. R. Komy and S. I. Abdelsalamd, Simultaneous effects of magnetic field and space porosity on compressible Maxwell fluid transport induced by a surface acoustic wave in a microchannel, Chin. Phys. B, 22, 124702 (2013).
[20] D. Tripathi, Study of transient peristaltic heat flow through a finite porous channel, Math. Comp. Mod., 57, 1270-1283 (2013).
[21] N. Ali, M. Sajid, T. Javed and Z. Abbas, Heat transfer analysis of peristaltic flow in a curved channel, Int. J. Heat Mass Transfer; 53, 3319-3325 (2010).
[22] Kh.S. Mekheimer, S. Z. A. Husseny and Y. Abd Elmaboud, Effects of heat transfer and space porosity on peristaltic flow in a vertical asymmetric channel, Numer. Meth. Partial Diff. Eqn. 26, 747-770 (2010).
[23] T. Hayat, F. M. Abbasi, B. Ahmad and A. Alsaedi, MHD mixed convection peristaltic flow with variable viscosity and thermal conductivity, Sains Malays., 43, 1583–1590 (2014).
[24] T. Hayat, F. M. Abbasi, M. Al-Yami and S. Monaquel, Slip and Joule heating effects in mixed convection peristaltic transport of nanofluid with Soret and Dufour effects, J. Mol. Liq., 194, 93-99 (2014).
[25] F. M. Abbasi, A. Alsaedi and T. Hayat, Peristaltic flow in an asymmetric channel with convective boundary conditions and Joule heating, J. Central South University, 21, 1411-1416 (2014).
[26] Fahad M. Abbasi, Tasawar Hayat, Sabir A. Shehzad, Fuad Alsaadi, Naif Altoaibi, Hydromagnetic peristaltic transport of copperwater nanofluid with temperature-dependent effective viscosity Particuology, 27 (2016) 133-140.
[27] F. M. Abbasi, T. Hayat, A. Alsaedi, Peristaltic transport of magneto-nanoparticles submerged in water: Model for drug delivery system, Physica E-Low-Dimensional Systems & Nanostructures, 68 (2015) 123-132.
[28] F. M. Abbasi, A. Alsaedi and T. Hayat, Mixed convective heat and mass transfer analysis for peristaltic transport in an asymmetric channel with Soret and Dufour effects, J. Cent. South Univ., 21, 4585-4591 (2014).
[29] F. M. Abbasi, T. Hayat and B. Ahmad, Peristaltic transport of copper-water nanofluid saturating porous medium, Physica E: Low-dimensional Systems and Nanostructures, 67, 47-53 (2015).

Fahad Munir Abbasi did his Ph.D. in Fluid Mechanics from Quaid-I-Azam University, Islamabad, Pakistan in 2014. Presently he is working as Assistant Professor at the Department of Mathematics, COMSATS Institute of Information Technology, Islamabad, Pakistan. His work mainly addresses the peristaltic flows of viscous and non-Newtonian fluids. Over the past couple of years, his work in the field of Newtonian and non-Newtonian fluid mechanics has been published extensively in the International Journals of good repute. He is among the promising young researchers of Pakistan.

Tasawar Hayat did his Ph.D. in applied mathematics from Quaid-I-Azam University, Islamabad, Pakistan in 1999. Since then, he has been in teaching and research at Quaid-I-Azam University, Islamabad, Pakistan. He joined as lecturer in 1998, and has been promoted to Professor. Besides that, he has been appointed as Distinguished National Professor by the Higher Commission of Pakistan. He has published extensively in Newtonian and non-Newtonian fluid mechanics. He has received a number of national and international awards, and is well known internationally.

Bashir Ahmad did his PhD from Quaid-I-Azam University, Islamabad, Pakistan in 1995. Presently he is serving as Professor at the Department of Mathematics, Faculty of Science, King Abdulaziz University, Jeddah, Saudi Arabia. His fields of interest include nonlinear ordinary differential equations, integro-differential equations, functional differential equations and fluid dynamics. He has published several articles in peer-reviewed journals. He is among the Hi-Ci researchers.